Curvature dark energy reconstruction through different cosmographic distance definitions

Salvatore Capozziello,[1,2,3,*] Mariafelicia De Laurentis,[1,2,4,†] and Orlando Luongo[1,2,5,‡]

[1] *Dipartimento di Fisica, Università di Napoli "Federico II", Via Cinthia, I-80126 Napoli, Italy.*
[2] *Istituto Nazionale di Fisica Nucleare (INFN), Sez. di Napoli, Via Cinthia, I-80126 Napoli, Italy.*
[3] *Gran Sasso Science Institute (INFN), Viale F. Crispi 7, I-67100 L'Aquila, Italy.*
[4] *Tomsk State Pedagogical University, 634061 Tomsk and National Research Tomsk State University, 634050 Tomsk, Russia.*
[5] *Instituto de Ciencias Nucleares, Universidad Nacional Autonoma de México (UNAM), Mexico.*

arXiv:1406.6996v1 [gr-qc] 26 Jun 2014

In the context of $f(\mathcal{R})$ gravity, dark energy is a geometrical fluid with negative equation of state. Since the function $f(\mathcal{R})$ is not known *a priori*, the need of a model independent reconstruction of its shape represents a relevant technique to determine which $f(\mathcal{R})$ model is really favored with respect to others. To this aim, we relate cosmography to a generic $f(\mathcal{R})$ and its derivatives in order to provide a model independent investigation at redshift $z \sim 0$. Our analysis is based on the use of three different cosmological distance definitions, in order to alleviate the duality problem, i.e. the problem of which cosmological distance to use with specific cosmic data sets. We therefore consider the luminosity, d_L, flux, d_F, and angular, d_A, distances and we find numerical constraints by the Union 2.1 supernovae compilation and measurement of baryonic acoustic oscillations, at $z_{BAO} = 0.35$. We notice that all distances reduce to the same expression, i.e. $d_{L;F;A} \sim \frac{1}{\mathcal{H}_0} z$, at first order. Thus, to fix the cosmographic series of observables, we impose the initial value of H_0 by fitting $\mathcal{H}_0$ through supernovae only, in the redshift regime $z < 0.4$. We find that the pressure of curvature dark energy fluid is slightly lower than the one related to the cosmological constant. This indicates that a possible evolving curvature dark energy realistically fills the current universe. Moreover, the combined use of d_L, d_F and d_A shows that the sign of the acceleration parameter agrees with theoretical bounds, while its variation, namely the jerk parameter, is compatible with $j_0 > 1$. Finally, we infer the functional form of $f(\mathcal{R})$ by means of a truncated polynomial approximation, in terms of fourth order scale factor $a(t)$.

PACS numbers: 98.80.-k, 98.80.Jk, 98.80.Es
Keywords: alternative theories of gravity; dark energy; cosmography; observational cosmology.

I. INTRODUCTION

Modern cosmology is nowadays plagued by several shortcomings which jeopardize the current understanding of universe dynamics. Particularly, these problems may suggest to reconsider the standard approach of gravitation, based on Einstein's gravity, in favor of alternative theories of gravity. Alternative gravity pictures have been extensively introduced in order to describe universe dynamics without the need of additional material ingredient as dark energy and dark matter described by new particles at fundamental level. On the other hand, the simple introduction of a cosmological constant vacuum energy seems inadequate to characterize the whole universe evolution at any epoch [1]. Thus, these alternative theories are viewed as a bid to reformulate *in toto* semi-classical schemes where General Relativity is only a particular case of a more extended theory. In particular, such theories are able to extend General Relativity predictions by means of higher order curvature invariants. Other pictures assume extensions based on minimally or non-minimally coupled scalar fields in the gravitational Lagrangians [2–6]. Furthermore, Einstein gravity can be extended by carrying out the full Mach principle: this fact leads to the introduction of a varying gravitational coupling. Under these hypotheses, the Brans-Dicke theory [7] represents the prototype of alternative schemes to General Relativity. It naturally includes a variable gravitational coupling, whose dynamics is governed by a single scalar field non-minimally coupled to geometry [7–9]. From one hand, extensions of General Relativity are therefore able to describe the above-mentioned theoretical aspects. On the other hand, it is also possible to account every unification scheme of fundamental interactions, such as superstring, supergravity, or grand unified theories and physically by low-energy effective actions containing non-minimal couplings or higher order curvature terms [10]. In fact, interactions between quantum scalar fields and background geometry, or gravitational self-interactions, naturally

*Electronic address: capozzie@na.infn.it
†Electronic address: felicia@na.infn.it
‡Electronic address: luongo@na.infn.it

yield such corrections to the Einstein-Hilbert's Lagrangian [11]. Hence, it is easy to show that several geometrical corrections are inescapable within quantum gravity effective actions and allow consistent pictures close to Planck scales [12]. These schemes represent working approaches towards a self consistent quantum picture, giving rise to interesting consequences once corrections like $\mathcal{R}^2$, $\mathcal{R}^{\mu\nu}$, $\mathcal{R}_{\mu\nu}$, $\mathcal{R}^{\mu\nu\alpha\beta}\mathcal{R}_{\mu\nu\alpha\beta}$, $\mathcal{R}\,\Box\mathcal{R}$, or $\mathcal{R}\,\Box^k\mathcal{R}$ are involved. A crucial fact is that alternative theories may provide analogies with the effective string or Kaluza-Klein Lagrangians, when compactification mechanisms of extra spatial dimensions are imposed [13].

A consequence of such extended theories of gravity is the possibility to frame current universe dynamics in a self consistent way considering their infrared counterpart. In particular, such models may address the problem of current universe speed up [14] by considering further gravitational degrees of freedom. Indeed, General Relativity seems not capable of dealing with present cosmic acceleration, unless an unknown fluid dubbed dark energy is added to the standard matter fluid energy-momentum tensor. At late times, the fluid responsible for accelerating the universe dominates over all other contributions, driving the universe evolution. It should be able to reproduce current observations [15]. Consequently, the dark energy equation of state behaves anti-gravitationally by counterbalancing gravitational attraction [16]. Thus, in this *concordance model*, the universe dynamics is described through pressureless matter terms, i.e. the sum of baryons and cold dark matter, through a evolving barotropic dark energy contribution and a vanishing spatial curvature $\Omega_k = 0$ [17, 18, 20].

A straightforward way to address geometrically the problem of dark energy is by the so called $f(\mathcal{R})$ gravity, where f is a generic function of the Ricci scalar $\mathcal{R}$ [4–6]. In this paper, we fix constraints on geometrical dark energy fluid inferred in the context of $f(\mathcal{R})$ gravity. To this end, we adopt cosmography to fix cosmological bounds on the $f(\mathcal{R})$ function and its derivatives at low redshift regime where degeneracy of concurring dark energy models is more evident. Cosmography allows to determine cosmological constraints in a model-independent way, once scalar curvature is somehow fixed. The idea is to expand into Taylor series cosmological observables. These expansions can be compared with data to get the cosmographic series, i.e. the numerical bounds on scale factor derivatives [21–23]. One commonly-used technique is represented by expanding the luminosity distance and compare it with supernovae data. However, a degeneration problem (duality problem) occurs once different cosmological distances are involved. Hence, a non-definitive consensus exists on the adequate cosmological distance to use in the framework of cosmography. We therefore perform the experimental analysis by means of three cosmological distance rulers, i.e. luminosity, flux and angular distances. We check the viability of different cosmological distances and measure cosmological constraints on the cosmographic series, deriving bounds on $f(\mathcal{R})$ curvature dark energy.

The paper is organized as follows: in Sec. II, we highlight the main features of cosmography and its application to cosmology. In Sec. III, we describe the problems related to cosmography, pointing out the so called duality problem. In Sec. IV, the experimental procedures is described. In Sec. V, cosmography in view of $f(\mathcal{R})$ is discussed . Finally, Sec. VI is devoted to conclusions and perspectives.

II. BASICS OF COSMOGRAPHY

Let us summarize the main aspects of cosmography and describe how it can be considered as a tool to fix constraints on cosmological observables. Firstly, let us assume that the cosmological principle holds and the equation of state is currently determined by a geometrical fluid, with pressure P_{curv}. Under these hypotheses, we expand cosmological observables into Taylor series and match the derivatives of such expansions with cosmological data. Examples of expanded quantities are the Hubble parameter, the luminosity distance, the apparent magnitude modulus [24, 25], the net pressure, and so forth [26, 27]. The power series coefficients of the scale factor expansion are known in the literature as *cosmographic series* (CS), if calculated at present time, or alternatively at the redshift $z = 0$. Those coefficients are therefore expressed in terms of the cosmological scale factor $a(t)$ and its derivatives [21]. It follows that the cosmographic approach does not need to assume a particular cosmological model.

Thence, one of the main advantage of cosmography is alleviating degeneracy among cosmological models, i.e. cosmography allows, in principle, to understand which model better behaves than others. In case of $f(\mathcal{R})$ gravity, for example, matter density degenerates with scalar curvature and cannot be constrained *a priori*. However, cosmography fixes model independent constraints on the cosmological equation of state and then results a technique to discriminate among competing $f(\mathcal{R})$ models [21], removing the degeneracy between matter and scalar curvature [22]. This technique turns out to be useful to reconstruct the form of $f(\mathcal{R})$ which better traces the universe expansion history. Thus, more precisely, cosmography represents a model independent method to infer cosmological bounds, once spatial curvature is somehow fixed.

Recent observations point out that the scalar curvature is negligible, so we can easily impose $\Omega_k = 0$ [28]. Than one has

$$\frac{1-a(t)}{H_0} \sim \Delta t + \frac{q_0}{2}H_0\Delta t^2 + \frac{j_0}{6}H_0^2\Delta t^3 - \frac{s_0}{24}H_0^3\Delta t^4 + \dots , \tag{1}$$

which represents the Taylor series of the scale factor $a(t)$, around $\Delta t = t - t_0 = 0$. The CS can be thus defined as

$$\frac{\dot{H}_0}{H_0^2} = -(1+q)\,, \quad \frac{\ddot{H}_0}{H_0^3} = j + 3q + 2\,, \quad \frac{H_0^{(3)}}{H_0^4} = s - 4j - 3q\,(q+4) - 6\,. \tag{2}$$

Here, dots represent derivatives with respect to the cosmic time t. Each term brings its own physical meaning. Particularly, the Hubble rate $H(t)$ is intimately related to the variation of $a(t)$ with time, the acceleration parameter $q(t)$ measures how the universe is speeding up and the jerk parameter $j(t)$ permits one to understand how the acceleration varied in the past. The coefficients are defined as

$$H(t) = \frac{1}{a}\frac{da}{dt}, \quad q(t) = -\frac{1}{aH^2}\frac{d^2a}{dt^2}, \quad j(t) = \frac{1}{aH^3}\frac{d^3a}{dt^3}\,, \tag{3}$$

and are considered at a given time t_0. We may argue that such quantities are able to describe the kinematics of the universe [29] and we do not pose, at this stage, the problem of which model causes the universe acceleration. In analogy to the classical mechanics, we say that cosmography is a kinematic approach to trace the universe expansion today. From one hand, the advantages of cosmography consist on its model independent reconstructions of present-time cosmology. In other words, it can be considered like a snapshot of the today observed universe capable of giving initial conditions for reconstructing back the cosmic evolution. From the other hand, the disadvantages rely on the fact that current data are either not enough to guarantee significative and accurate constraints or do not fit significant intervals of convergence for $z \ll 1$. In addition, the cosmological observable that one expands into Taylor series, i.e. $a(t)$ is not known *a priori*. Consequently, there is no physical motivations to use a particular cosmological distance than others. This means that the use of a given luminosity distance to constrain CS is only motivated by *ad hoc* arguments. This fact constitutes the so-called *duality problem* that we discuss in the next section. To alleviate duality problem, we will compare three different cosmological distances to trace universe expansion history at late times, under the hypothesis of a $f(\mathcal{R})$ geometrical dark energy fluid.

III. THE DUALITY PROBLEM AND COSMOGRAPHIC CONVERGENCE

By a cosmographic analysis, one can fix constraints on the geometrical dark fluid, alleviating the degeneracy problem. To this end, one needs a self-consistent definition of causal distance. Unfortunately, standard definitions implicitly postulate that the universe is accelerating [30, 31], i.e. to infer the distance expansion, we evaluate the distance r_0 that a photon travels from a light source at $r = r_0$ to our position at $r = 0$, defined as $r_0 = \int_t^{t_0} \frac{dt'}{a(t')}$. Consequently, one obtains as prototype the so called luminosity distance d_L, while other definitions, e.g. the photon flux distance d_F, angular diameter distance d_A and so forth, can easily be derived from different considerations. As previously stressed, this leads to a severe duality problem on the choice of the particular cosmological ruler to use for fixing cosmological constraints on the CS.

Here, we use three different cosmological distances as rulers, e.g. the luminosity, flux and angular distances, d_L, d_F and d_A respectively. Below the definition of these distances is reported in terms of r_0, that is

$$d_L = a_0 r_0 (1+z) = r_0\, a(t)^{-1}\,, \tag{4a}$$

$$d_F = \frac{d_L}{(1+z)^{1/2}} = r_0\, a(t)^{-\frac{1}{2}}\,, \tag{4b}$$

$$d_A = \frac{d_L}{(1+z)^2} = r_0\, a(t)\,. \tag{4c}$$

These distances can be used to the fix causal constraints on the curvature fluid in order to alleviate the degeneracy problem. For the sake of clearness, it is important to stress that although d_L is associated to the ratio of the apparent and absolute luminosity of astrophysical objects, the other distances, i.e. d_F and d_A, may be also used to fix bounds on the observable universe. All the different cosmological distances rely on the fundamental assumption that the total number of photons is conserved at cosmic scales. Hence, there is no reason to discard one distance with respect to another since all of them fulfill this condition. The duality problem represents a not well understood issue of observational cosmology [32]. In this work, we find differences in fitting Eqs. (4), showing that there is no reason to adopt d_L only as the only cosmological distance.

However a problem of *convergence* may occur, leading to possible misleading results for $z > 1$ in the cosmographic Taylor series. An immediate example is due to the most high supernova redshift in a typical data set. Usually, one

has that the furthest redshift at approximatively $z \sim 1.41$, showing that a few number of supernovas spans in the range $z > 1$. It follows that numerical divergences and bad convergences may occur in the analysis, since Taylor expansions are carried out around $z = 0$. A plausible landscape deals with introducing alternative redshift definitions, re-parameterizing the cosmological distances in a tighter redshift range [33]. These possible re-parameterizations must fulfill the conditions that the distance curves should not behave too steeply in the interval $z < 1$. Moreover, the luminosity distance curve should not exhibit sudden flexes, being one-to-one invertible as discussed in [21]. In other words, it is easy to show that the new redshift re-parameterization, i.e. z_{new}, provides $z_{new} = \mathcal{Z}(z)$, with $\mathcal{Z}$ a generic function of the redshift z, with the property $\mathcal{Z} \to 1$, as $z \to \infty$. In this work, we describe a technique to reduce the convergence problem, calibrating cosmological distance at first order in the Taylor series within a smaller range of redshift. Our strategy is to fix H_0 with supernovae in the range $z < 0.4$. This turns out to be useful since a wide range of data is actually inside the sphere $z < 1$ and all cosmological distances at first order reduce to

$$d_i \sim \frac{z}{H_0}\,, \tag{5}$$

where d_i represents the generic distance, i.e. $i = L; F; A$. Once H_0 is fixed, the series naturally converges better since its shape increases or decreases as H_0 decreases or increases respectively. In other words, the dynamical shape of any cosmological curve depends on the value given to H_0. As H_0 is somehow known, curves behave better at higher redshift, alleviating convergence problems as expected. These arguments represent a further tool in order to fix model independent constraints on $f(\mathcal{R}(z))$ and its derivatives. Indeed, H_0 is fixed regardless the cosmological distance taken into account, by means of Eq. (5). It is possible to fix H_0 in the range $z < 0.4$ with supernovae only. We find

$$H_0 = 69.785^{+1.060}_{-1.040}\,. \tag{6}$$

In cosmography, the strategy of fixing H_0 in a smaller interval of data overcomes several problems associated to the well consolidated usage of auxiliary variables. Indeed, as above mentioned, the method of adopting auxiliary variables consists in determining parametric functions $y(z)$ in terms of the redshift z, whose values rely in the interval $y(z) \in [0, 1]$, as $z \to 0$ and $z \to \infty$ respectively. This procedure rearranges catalog data and suffers from severe shortcomings [33, 34]. Indeed, the form of $y(z)$ is not known *a priori* and any possible reparameterized variable should guarantee that errors do not deeply propagate in the statistical analysis. In several cases, $y(z)$ variables are therefore inconsistent with low redshift cosmography, providing misleading results, albeit their use becomes more relevant for high redshift data sets.

In our case, we propose to fix H_0 as a *low redshift cosmographic setting value*, since all distances reduce to Eq. (5) at a first order of Taylor expansions. Our corresponding best fit intervals are compatible with previous analysis [35] and guarantee that errors do not significatively propagate on measured coefficients. For our purposes, the strategy of fixing H_0 by means of small redshift data only better behaves than standard auxiliary variables, due to the fact that $z \leq 1$ (see for recent applications [36–38]), although it would fail at higher redshift domains. Since, in our cases, z reaches the upper value $z \sim 1.414$, i.e. the maximum z of the supernova compilation, we expect that the use of Eq. (5) to get H_0 would guarantee refined best fit results with respect to any possible reparameterized auxiliary variables.

An additional technique is to combine more than one data set to infer cosmological bounds. Indeed, although we treat bad convergence of truncated series by using Eq. (6), further data sets would improve the quality of numerical estimates. Hence, the CS and the derived constraints on $f(\mathcal{R})$ derivatives would improve consequently. Here, we combine supernovae data with the baryonic acoustic oscillation measurement. It is possible to show that such a choice actually reduces the convergence problem.

IV. COSMOLOGICAL DATA SETS AND THE FITTING PROCEDURE

In this section, we describe the two data sets used for the cosmographic analysis. First, let us consider the Union 2.1 compilation [39]. Second, we assume the measurement of baryonic acoustic oscillation (BAO) [40]. As it is well known, supernovae data span in the plane $\mu - z$, consisting of 580 supernovae, in the observable range $0.015 < z < 1.414$. For our purposes, to fix viable constraints, we follow a standard Bayesian analysis, dealing with the determination of best fits, evaluated by maximizing the likelihood function $\mathcal{L} \propto \exp(-\chi^2/2)$. Here, χ^2 is the *(pseudo)*χ*-squared* function, or reduced χ squared. The distance modulus μ for each supernova is

$$\mu = 25 + 5\log_{10}\frac{d_L}{Mpc}\,, \tag{7}$$

and once given the corresponding σ_i error, we are able to minimize the χ square as follows

$$\chi^2_{SN} = \sum_i \frac{(\mu_i^{\rm theor} - \mu_i^{\rm obs})^2}{\sigma_i^2}\,. \tag{8}$$

On the other hand, the large scale galaxy clustering observations provide the signatures for the baryonic acoustic oscillation. This gives a further tool to explore the parameter space and alleviate the convergence problem. We use the peak measurement of luminous red galaxies observed in Sloan Digital Sky Survey (SDSS). By employing $\mathcal{A}$ as the measured quantity, we have

$$\mathcal{A} = \sqrt{\Omega_m}\Big[\frac{H_0}{H(z_{BAO})}\Big]^{\frac{1}{3}}\left[\frac{1}{z_{BAO}}\int_0^{z_{BAO}}\frac{H_0}{H(z)}dz\right]^{\frac{2}{3}}\,, \tag{9}$$

with $z_{BAO} = 0.35$. In addition, the observed $\mathcal{A}$ is estimated to be $\mathcal{A}_{obs} = 0.469\,\big(\frac{0.95}{0.98}\big)^{-0.35}$, with an error $\sigma_{\mathcal{A}} = 0.017$. In the case of the BAO measurement, we minimize the χ squared

$$\chi^2_{BAO} = \frac{1}{\nu}\left(\frac{\mathcal{A} - \mathcal{A}_{obs}}{\sigma_{\mathcal{A}}}\right)^2\,. \tag{10}$$

An important feature of BAO is that it does not depend on H_0.

Estimations of the cosmographic parameters may be performed passing through the standard Bayesian technique, maximizing the likelihood function:

$$\mathcal{L}_i \propto \exp(-\chi^2_i/2)\,, \tag{11}$$

where χ^2_i is explicitly determined for each compilations here employed and the subscript indicates the data set, i.e. supernovae or BAO. Maximizing the likelihood function is equivalent to minimizing the total $\chi_t \equiv \chi_{SN} + \chi_{BAO}$-squared function and so one argues to maximize

$$\mathcal{L}_{tot} \equiv \mathcal{L}_{SN} \times \mathcal{L}_{BAO} \propto \exp(-\chi^2_t/2)\,. \tag{12}$$

In particular, the cosmographic results have been obtained by directly employing Eq. (12) maximizing the corresponding likelihood functions over a grid, through a standard Bayesian analysis. In so doing, the cosmographic series has been evaluated and the provided errors refer to as the $1\,\sigma$, associated to the 68% of confidence level. Once all cosmographic coefficients have been determined through a direct Gaussian maximization of the likelihood function, we will infer the derived coefficients, $f_0, f_{z0}, f_{zz0}, P_{curv}$, by simply propagating the errors through the well consolidated logarithmic method.

V. $f(\mathcal{R})$ COSMOGRAPHY VS REDSHIFT

Let us consider now the $f(\mathcal{R})$ coefficients (evaluated in terms of the redshift z) as function of observable quantities. The robustness of calculations leads to the advantage of relating derivatives of $f(\mathcal{R}(z))$ at $z = 0$ to experimental bounds, without assuming a priori a form of $f(\mathcal{R}(z))$. Hence, by expanding the causal distances d_L, d_F and d_A, through the definition of the scale factor in terms of redshift, $a \equiv (1+z)^{-1}$, we get

$$\begin{aligned} d_L \;=\; & \frac{1}{H_0}\cdot\Big[z + z^2\cdot\Big(\frac{1}{2} - \frac{q_0}{2}\Big) + z^3\cdot\Big(-\frac{1}{6} - \frac{j_0}{6} + \frac{q_0}{6} + \frac{q_0^2}{2}\Big) + \\ & + z^4\cdot\Big(\frac{1}{12} + \frac{5j_0}{24} - \frac{q_0}{12} + \frac{5j_0q_0}{12} - \frac{5q_0^2}{8} - \frac{5q_0^3}{8} + \frac{s_0}{24}\Big) + \ldots\Big]\,, \end{aligned}$$

$$\begin{aligned} d_F \;=\; & \frac{1}{H_0}\cdot\Big[z - z^2\cdot\frac{q_0}{2} + z^3\cdot\Big(-\frac{1}{24} - \frac{j_0}{6} + \frac{5q_0}{12} + \frac{q_0^2}{2}\Big) + \\ & + z^4\cdot\Big(\frac{1}{24} + \frac{7j_0}{24} - \frac{17q_0}{48} + \frac{5j_0q_0}{12} - \frac{7q_0^2}{8} - \frac{5q_0^3}{8} + \frac{s_0}{24}\Big) + \ldots\Big]\,, \end{aligned}$$

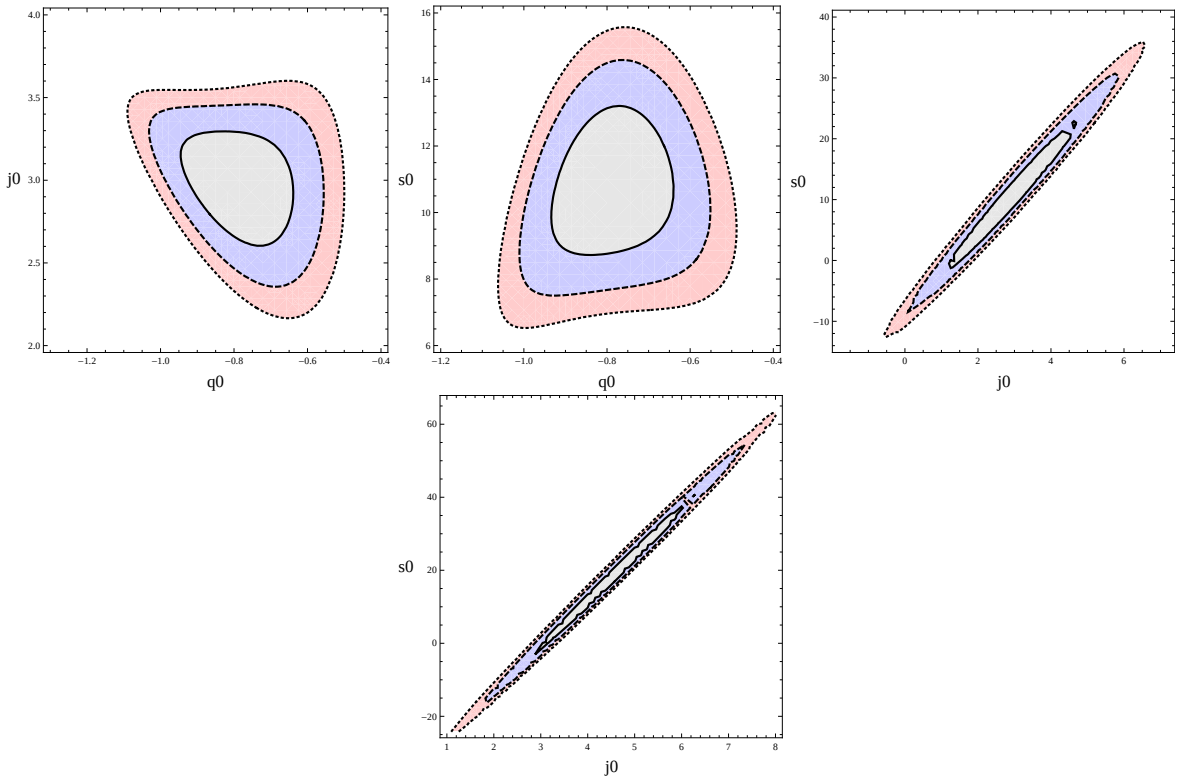

FIG. 1: Contour plous derived from fitting procedures. Above, as examples, we report the first three contour plots, obtained by using the luminosity distance and the last plot, derived from the use of d_F. Each plot shows the 68%, 95% and 99% of confidence levels. Easily one can notice that there are some difficulties in bounding q_0 versus j_0, as reported in Tables I and II, with 1σ error bars.

and

$$d_A = \frac{1}{H_0}\cdot\left[z+z^2\cdot\left(-\frac{3}{2}-\frac{q_0}{2}\right)+z^3\cdot\left(\frac{11}{6}-\frac{j_0}{6}+\frac{7q_0}{6}+\frac{q_0^2}{2}\right)+\right.$$
$$\left.+z^4\cdot\left(-\frac{25}{12}+\frac{13j_0}{24}-\frac{23q_0}{12}+\frac{5j_0q_0}{12}-\frac{13q_0^2}{8}-\frac{5q_0^3}{8}+\frac{s_0}{24}\right)+\dots\right].$$

Thus, by considering the redshift definition in terms of the cosmic time $\dfrac{d\log(1+z)}{dt} = -H(z)$, we can rewrite $\mathcal{R}$ as a function of z, being

$$\mathcal{R} = 6\left[(1+z)H\,H_z - 2H^2\right]. \tag{13}$$

Hence, it is now easy to get $\mathcal{R}$ and derivatives in terms of z, and to evaluate the corresponding values at present time. We obtain

$$\mathcal{R}_0 = 6H_0\left[H_{z0}-2H_0\right], \quad \mathcal{R}_{z0} = 6H_{z0}^2 + H_0(-3H_{z0}+H_{2z0}), \tag{14}$$

that, for present time, simply allow us to write

$$H_{z0} = H_0(1+q_0),$$
$$H_{2z0} = H_0(j_0-q_0^2),$$
$$H_{3z0} = H_0(-3j_0-4j_0q_0+q_0^2+3q_0^3-s_0),$$

where derivatives with respect to z are indicated. By assuming the presence of standard pressureless matter, ($\rho_m \propto a^{-3}$ and $P_m = 0$), including baryons and cold dark matter, the modified Friedmann equation, which fixes the whole energy

TABLE I: Table of supernovae best fits with 1σ error bars.

Parameter	d_L	d_F	d_A
	$\chi^2_{min} = 0.9764$	$\chi^2_{min} = 0.9812$	$\chi^2_{min} = 0.9832$
q_0	$-0.791^{+0.151}_{-0.131}$	$-1.590^{+0.109}_{-0.108}$	$-1.645^{+0.112}_{-0.112}$
j_0	$2.981^{+0.334}_{-0.312}$	$4.552^{+0.791}_{-0.780}$	$4.659^{+0.757}_{-0.803}$
s_0	$10.878^{+2.295}_{-2.103}$	$18.526^{+2.121}_{-1.960}$	$19.523^{+4.274}_{-3.356}$
$P_{curv,0}$	$-1.986 \div -0.687$	$-1.886 \div -0.722$	$-1.984 \div -0.789$
f_0	$-5.844 \div -5.280$	$-7.397 \div -6.963$	$-7.514 \div -7.066$
f_{z0}	$9.546 \div 11.730$	$20.822 \div 28.946$	$21.678 \div 29.694$
f_{2z0}	$-102.728 \div -59.785$	$-116.976 \div -77.479$	$-133.166 \div -72.456$

The range of measurements are inferred through the logarithmic formula, once the CS is fitted and Eqs. (18) assumed.

budget of the universe, easily reads

$$H^2 = \frac{1}{3}\left[\rho_{curv} + \frac{\rho_m}{f'(\mathcal{R})}\right], \tag{15}$$

with the dynamical expression for H, i.e. $2\dot{H} + 3H^2 = -P_{curv}$. Eq. (15) determines curvature corrections from which we infer the dark energy fluid. In other words, the fluid density, responsible for the cosmic speed up, could be rewritten as

$$\rho_{curv} = \frac{1}{f'(\mathcal{R})}\left\{\frac{1}{2}\Big[f(\mathcal{R}) - \mathcal{R}f'(\mathcal{R})\Big] - 3H\dot{\mathcal{R}}f''(\mathcal{R})\right\}, \tag{16}$$

with the corresponding curvature pressure

$$\frac{P_{curv}}{\rho_{curv}} = w_{curv} = -\left(1 - \frac{\ddot{\mathcal{R}}f''(\mathcal{R}) + \dot{\mathcal{R}}\left[\dot{\mathcal{R}}f'''(\mathcal{R}) - Hf''(\mathcal{R})\right]}{\left[f(\mathcal{R}) - \mathcal{R}f'(\mathcal{R})\right]/2 - 3H\dot{\mathcal{R}}f''(\mathcal{R})}\right). \tag{17}$$

It is convenient, for our purposes, to work in terms of $f(z)$, i.e. the $f(\mathcal{R})$ explicitly depending on the redshift z. In so doing, we assume the functional dependence $\mathcal{R} = \mathcal{R}(z)$, and find $f'(\mathcal{R}) = \mathcal{R}_z^{-1} f_z$, $f''(\mathcal{R}) = (f_{2z}\mathcal{R}_z - f_z\mathcal{R}_{2z})\mathcal{R}_z^{-3}$. As it is discussed in [22, 41], $f(\mathcal{R})$ models have to evade Solar System tests for General Relativity. This means that gravitational coupling has to agree with the local observed value. This is possible if the conditions

$$f_0 = 2H_0^2(q_0 - 2), \quad f_{z0} = 6H_0^2(j_0 - q_0 - 2), \quad f_{2z0} = -6H_0^2\Big[s_0 + 4q_0 + (2 + q_0)j_0 + 2\Big], \tag{18}$$

hold. From Eqs. (18), numerical estimates are derived once the CS is known from model independent fitting procedures by means of Eqs. (4). The numerical results of our analysis are reported in Tab. I and II. They have been obtained by employing numerical outcomes for $\mathcal{H}_0$, determined by the use of Eq. (13).

Our results indicate a slightly lower dark energy pressure than the one predicted by ΛCDM model, which typically is $P_{\Lambda CDM} \sim -0.7$. This fact suggests that any curvature dark energy fluid should behave differently than a pure (effective) cosmological constant. In general, numerical outcomes for P_{curv} does not completely agree with ΛCDM but give compatible acceleration parameters for d_L.

However, our results show that present data are not enough to completely constrain possible violations of the duality problem. Even though it is difficult to definitively remove such a problem, our approach allows one to alleviate it by dealing with the BAO measurement as a Gaussian prior in the likelihood definition. In so doing, one significantly reduces the allowed phase space, circumscribing Gaussian errors and reducing any possible systematics. This procedure has been accurately investigated also with different typologies of priors [35]. In particular, through general analyses carried out by means of Monte Carlo Markov chains, it seems that more stringent intervals occur as the BAO measurement is included [42]. Such tighter best fit values are however not incompatible with our results which rely in viable cosmographic intervals [33–36]. More stringent values will be carried out through Monte Carlo approaches, also in the field of $f(\mathcal{R})$ gravity, as one can notice from first confirmations in [41]. In addition, all

TABLE II: Table of supernovae+BAO best fits with 1σ error bars.

Parameter	d_L $\chi^2_{min} = 0.9704$	d_F $\chi^2_{min} = 0.9795$	d_A $\chi^2_{min} = 0.9796$
q_0	$-0.688^{+0.124}_{-0.122}$	$-1.216^{+0.137}_{-0.133}$	$-1.456^{+0.142}_{-0.139}$
j_0	$2.126^{+0.412}_{-0.397}$	$3.486^{+0.821}_{-0.811}$	$3.744^{+0.792}_{-0.786}$
s_0	$10.878^{+2.295}_{-2.103}$	$18.526^{+2.121}_{-1.960}$	$19.523^{+4.274}_{-3.356}$
$P_{curv,0}$	$-1.677 \div -0.725$	$-1.6626 \div -0.724$	$-1.696 \div -0.758$
f_0	$-5.620 \div -5.128$	$-6.698 \div -6.158$	$-7.190 \div -6.628$
f_{z0}	$3.234 \div 6.612$	$12.144 \div 20.316$	$15.318 \div 23.100$
f_{2z0}	$-99.369 \div -57.555$	$-133.786 \div -89.469$	$-141.916 \div -77.910$

The range of measurements are inferred through the logarithmic formula, once the CS is fitted and Eqs. (18) assumed.

cosmological distances indicate a positive, greater than 1, jerk parameter j_0, although they provide unexpectedly smaller acceleration parameters for d_F and d_A distances.

The statistical strategy adopted to find out our cosmographic results permits one to immediately get the requested values for q_0, j_0, s_0. Our results are actually statistically consistent, as one argues from the corresponding chi square functions and $1\,\sigma$ errors. Those results remarkably show that j_0 and s_0 increase, as the acceleration parameter q_0 decreases and confirm previous studies on the cosmographic series, providing intervals of confidence in agreement with theoretical predictions. However, although all χ square parameters are nearly the same for all the fits involved, the leading results determined from d_L better support theoretical predictions, since seem to be more compatible with a higher acceleration parameters, as one expects from current data [15, 33, 34, 43].

$$f_0 < 0\,, \quad f_{z0} > 0\,, \quad f_{2z0} < 0\,, \quad P_{curv} < P_{\Lambda CDM}\,. \tag{19}$$

Summing up, the absolute values of each variable increases as one performs fits with d_F and d_A. In other words, d_F and d_A analyses show significative departures, incompatible to the values found by d_L, for the CS, although they indicate compatible values of f_0, f_{z0} and f_{2z0} and give reasonable agreement with P_{curv}.

Keeping in mind such considerations, we are therefore able to infer the functional form of $f(z)$, *compatible* with previous results. In particular, we get

$$f(z) \sim -\left(a + \sum_{i=0}^{\mathcal{N}} a^{-i^2}\right) + \mathcal{O}(z)\,, \tag{20}$$

where $a \equiv (1+z)^{-1}$, with $\mathcal{N}$ a truncating number, i.e. $\mathcal{N} \sim 4$. The approach fulfills the cosmographic bounds and gives reasonable results for $f(\mathcal{R})$ reconstructions (see also [41]). In particular, $f(0) < 0$ and the statistically favored dependence of $f(z)$ on z is an inverse series in terms of z.

VI. DISCUSSION AND CONCLUSIONS

In this paper, we present a method to fix constraints on *curvature dark energy* in the context of $f(\mathcal{R})$ gravity by using a cosmographic analysis derived from different cosmological distances. Cosmography is here adopted to determine model independent bounds on observables related to $f(\mathcal{R})$ and its derivatives. We follow this procedure by keeping in mind that each term of CS has a precise physical meaning, and allows to infer dynamical properties of $f(\mathcal{R})$ curvature fluid. Rephrasing this point, the limits on CS allow to recover present time bounds on the dark energy dynamics, regardless the particular cosmological model. In so doing, to alleviate the duality problem among cosmological distances, we investigate cosmography by means of the luminosity, flux and angular distances. The approach consists in using cosmography to fix cosmological bounds on curvature fluid and to choose a combination of causal distances in order to alleviate degeneracy among cosmological models. Determining cosmographic results through the three mentioned distances leads to tighter intervals of measurements, showing that values of curvature dark energy pressure rely in lower bounds than the intervals expected in a pure ΛCDM model. To this end, we used

two data sets, i.e. the Union 2.1 compilation of supernovae and the baryonic acoustic oscillation measurements. In our analysis, we considered the today observed value of the Hubble parameter H_0 as a prior. This choice is due to the need of alleviating the convergence problem which plagues cosmography as soon as cosmological data exceed the range $z > 1$. Thus, we fix H_0 as a sort of *initial condition* on the three distances, by means of supernovae only, using all the distances expanded at the lowest order of z, that is $d_{L;F;A} \sim \frac{1}{H_0} z$. The corresponding fitting value of H_0 has been obtained in the supernovae range $z < 0.4$ where the convergence problem does not exist. This technique is developed in order to determine better the values of q_0, j_0 and s_0, without introducing any re-parametrization variable of the redshift. In addition, we get constraints on $f(z)$ derivatives up to the second order in the Taylor expansion around $z = 0$ and found that the acceleration parameter q_0 is almost compatible when inferred from d_L while the jerk and snap parameters are only compatible with $j_0 \geq 1$, $s_0 > 1$ respectively. These outcomes indicate again that the standard cosmological paradigm, namely the ΛCDM model, may be extended in terms of curvature dark energy fluid. Finally, we proposed, as test function, a particular $f(z)$, able to reproduce the cosmographic bounds that fairly well fits the Hubble diagram up to fourth order expansion in powers of $a(t)$. In future research, we will refine this approach by combining more cosmological tests and further distances. This approach will allow to reduce the phase spaces and better constrain the free parameters of curvature dark energy.

[1] Peebles, P. J. E., Ratra, B., Rev. Mod. Phys., **75**, (2003).
[2] Capozziello, S., Int. J. Mod. Phys. **D 11**, 483 (2002).
[3] Nojiri S., Odintsov S.D., Int. J. Geom. Meth. Mod. Phys., **4**, 115, (2007).
[4] Capozziello, S., Francaviglia, M., Gen. Rel. Grav., **40**, 357, (2008).
[5] Capozziello, S., De Laurentis, M., Phys. Rept., **509**, 167, (2011).
[6] Nojiri, S., Odintsov, S. D., Phys. Rept., **505**, 59, (2011).
[7] Brans, C. H., Dicke, R. H., Phys. Rev., **124**, 925, (1961).
[8] Capozziello, S., de Ritis, R., Rubano, C., Scudellaro, P. Nuovo Cimento, **4**, 19, (1996).
[9] Buchbinder, I. L., Odintsov, S. D., Shapiro, I. L., *Effective Action in Quantum Gravity*, IOP Publishing, Bristol, (1992).
[10] Sciama, D. W., Mon. Not. R. Ast. Soc., **113**, 34, (1993).
[11] Birrell, N. D., Davies, P. C. W., *Quantum Fields in Curved Space*, Cambridge University Press, Cambridge, (1982).
[12] Vilkovisky, G. *Effective action in quantum gravity*, Class. Quant. Grav., **9**, 895, 1992.
[13] Gasperini, M., Veneziano, G., Phys. Lett. B, **277**, 256, (1992).
[14] Riess, A. G., et al., AJ, **116**, 1009, (1998); Perlmutter, S., et al., ApJ, **517**, 565, (1999).
[15] Capozziello, S., De Laurentis, M. Luongo, O., Ruggeri, A. C., Galaxies 2013, 1(3), 216-260;
[16] Luongo, O., Quevedo, H., arXiv:1005.4532, (2010).
[17] Bamba, K., Capozziello, S., Nojiri, S., Odintsov, S. D., Astrophys. Space Sci., **342**, 155-228, (2012).
[18] Li, M., Li, X., Wang, S., Zhang, X., JCAP, 0906, **036**, (2009);
[19] Linder, E., Gen. Rel. Grav., **40**, 23, (2008).
[20] Copeland, E. J., Sami, M., Tsujikawa, S., Int. J. Mod. Phys. D, **15**, 1753-1936, (2006).
[21] Aviles, A., Gruber, C., Luongo, O., Quevedo, H., Phys. Rev. D, **86**, 123516, (2012).
[22] Capozziello, S., Cardone, V.F., Salzano, V., Phys.Rev. D **78**, 063504 (2008).
[23] Capozziello, S., Lazkoz, R., Salzano, V., Phys.Rev. D **84**, 124061 (2011).
[24] Luongo, O., Mod. Phys. Lett. A, **26**, 20, 1459-1466 (2011).
[25] Demianski, M., Piedipalumbo, E., Rubano, C., Scudellaro, P., Month. Not. of the Roy. Astr. Soc., **426**, 1396-1415, (2012); Luongo, O., Iannone, G., Autieri, C., Europh. Lett. **90**, 39001, (2010).
[26] Lavaux, G., Wandelt, B. D., Astr. Jour., **754**, 109, (2012); Aviles, A., Bonanno, L., Luongo, O., Quevedo, H., Phys. Rev. D, **84**, 103520, (2011); Iannone, G., Luongo, O., Europh. Lett., **94**, 49002, (2011).
[27] Gruber, C., Luongo, O., Phys. Rev. D, **89**, 103506, (2014).
[28] Mennella, A., et al. A & A, **536**, 3, (2011); Verde, L., Protopapas, P., Jimenez R., ArXiv[astro-ph]: 1306.6766, (2013).
[29] Neben, A. R., Turner, M. S., ApJ, **769**, 133, (2013).
[30] Nair, R., Jhingan, S., Jain, O., JCAP, **12**, 028, (2012).
[31] Holanda, R. F. L., Goncalves, R. S., Alcaniz, J. S., JCAP, **1206**, 022, (2012).
[32] Etherington, I. M. H., Gen. Rel. Grav., **39**, 1055, (2007).
[33] Aviles, A., Gruber, C., Luongo, O., Quevedo, H., arXiv[gr-qc]:1301.4044, (2013); Cattoen, C. Visser, M. Phys. Rev. D, **78**, 063501, (2008); Luongo, O., Quevedo, H., Astroph. and Sp. Sci., **338**, 2, 345-349 (2012); Cattoen, C., Visser, M., ArXiv[gr-qc]:0703122, (2007); Xu, L., Wang, Y., Phys. Lett. B, **702**, 114, (2011).
[34] Visser, M., Class. Quant. Grav., **21**, 2603-2616, (2004).
[35] Nesseris, S., Garca-Bellido, J., Phys. Rev. D, **88**, 063521, (2013); Bochner, B., Pappas, D., Dong, M., ArXiv[astro-ph]:1308.6050, (2013).
[36] Aviles, A., Bravetti, A., Capozziello, S., Luongo, O., ArXiv[gr-qc]:1405.6935, (2014).
[37] Demianski, M., Piedipalumbo, E., Rubano, C., Scudellaro, P., Mon. Not. Roy. Astr. Soc., **426**, 1396-1415 (2012).

[38] Capozziello, S., Farooq, O., Luongo, O., Ratra, B., ArXiv[gr-qc]:1403.1421, (2014).
[39] Komatsu, E., et al., Astrop. J. Sup., **192**, 18, (2011).
[40] Percival, W. J., et al., Mon. Not. Roy. Astron. Soc., **381**, 1053, (2007).
[41] Aviles, A., Bravetti, A., Capozziello, S., Luongo, O., Phys. Rev. D, **87**, 044012, (2013).
[42] Lazkoz, R., Alcaniz, J., Escamilla-Rivera, C., Salzano, V., Sendra, I., JCAP, **12**, 005, (2013).
[43] Jun-Qing; X., Vitagliano, V., Liberati, S., Viel, M., Phys. Rev. D, **85**, 043520, (2012).